Northumbria Research Link

A comprehensive design and optimization of an offset strip-fin compact heat exchanger for energy recovery systems

Muhammad Ahmad Jamil [a,b], Talha S. Goraya [b], Asad Ur Rehman [b], Haseeb Yaqoob [b], Muhammad Ikhlaq [c], Muhammad Wakil Shahzad [a,*], Syed M. Zubair [d,*]

[a] Mechanical & Construction Engineering Department, Northumbria University, Newcastle Upon Tyne NE1 8ST, United Kingdom
[b] Department of Mechanical Engineering, Khwaja Fareed University of Engineering and Information Technology, Rahim Yar Khan, Pakistan
[c] School of Engineering, Merz Court, Newcastle University, Newcastle Upon Tyne NE1 7RU, United Kingdom
[d] Mechanical Engineering Department, King Fahd University of Petroleum & Minerals, KFUPM Box # 1474, Dhahran 31261, Saudi Arabia

ARTICLE INFO

ABSTRACT

Energy recovery in conventional thermal systems like power plants, refrigeration systems, and air conditioning systems has enhanced their thermodynamic and economic performance. In this regard, compact heat exchangers are the most employed for gas to gas energy recovery because of their better thermal performance. This paper presents an economic optimization of a crossflow plate-fin heat exchanger with offset strip fins. A detailed software-based numerical code for thermal, hydraulic, economic, and exergy analysis is developed for three fin geometries. Genetic Algorithm, parametric, and normalized sensitivity analyses are used to discover the most influential parameters to optimize the total cost. The parametric study showed that with the increase of mass flow rates and plate spacing, outlet stream cost and operating cost increased due to the rise in pressure drops. Finally, the optimization reduced the operational cost by ~78.5%, stream cost by ~64.5%, and total cost by ~76.8%.

Introduction

Heat exchangers are the backbone of energy recovery systems and have been focused on growing concerns over energy conservation and efficient systems design. Particularly, the compact heat exchangers (CHEs) have attained significant attention due to the larger heat exchanger surface area per unit volume. The two main types of these heat exchangers are the tube-fin heat exchangers and the plate-fin heat exchangers (PFHEs) [1]. The PFHEs are preferred in liquefaction plants [2], air separation [3], cryogenic applications [4,5], aerospace [6], and petrochemical [7] industries because of high thermal effectiveness, compact size, and lightweight [8]. Therefore, significant research has been conducted to analyze these heat exchangers.

For instance, Saggu et al. [5] analyzed the fin reliability of a PFHE in liquefied natural gas (LNG) applications. They employed finite element analysis to the brazed joint stress produced by the high-temperature

gradient and reported that the stress in the upper face is reduced by 18%. Nuňez et al. [9] studied the surface selection designs of PFHEs. They presented a new design algorithm based on the volume performance index that offered a direct solution to the sizing of PFHEs, unlike the traditional design procedures. Wen and Li [10] proposed the installation of baffles in the header for improved fluid flow distribution that enhanced the heat exchanger performance by reducing the flow maldistribution parameters from 0.95 to 0.32. Yang and Li [11] reported that geometrical attributes like fin dimensions and fin-channel characteristics considerably affect the overall heat exchanger performance. They also proposed a correlation and stated that it predicts 92.5% of the Colburn factor (*j*) data and 90.3% of the Fanning friction factor (*f*) data within 20%, with less than 15% RMS errors. Aliabadi et al. [12] analyzed corrugated plate-fin (CPF) and vortex generator plate-fin (VGPF) heat exchangers and proposed a new design for enhanced performance. They reported that the proposed method had 76.6% higher Nu for the CPF channel and 53.2% for the VGPF channel compared to

Nomenclature

A	heat transfer area, m^2
A_f	fin area, m^2
BP	blowing/pumping power, kW
b	plate spacing/fin height, m
C^*	heat capacity ratio
$\dot{C}$	product cost, ($/h)
C_{ele}	cost of electricity, $/kWh
C_{index}	cost index factor
C_{inv}	investment cost
C_o	annual current cost, $/y
C_{op}/C_{opc}	operational cost
C_p	specific heat capacity, J/kg.K
C_{total}	the total cost of equipment, $
D	diameter, m
D_h	hydraulic diameter, m
$\overline{ex}$	specific exergy, k.J/kg
f	Fanning friction factor
G	mass flux, kg/s m^2
h	heat transfer coefficient, W/m^2.K
$h^{'}$	enthalpy, kJ
$H^{'}$	difference between fin height and fin metal thickness, m
i	interest rate, %
j	Colburn Factor
K	thermal conductivity, W/m.K
$K^{'}$	reference cost constant
L_1	hot flow length of the heat exchanger, m
L_2	cold flow length of the heat exchanger, m
L_3	non-flow length of the heat exchanger, m
l_s	fin offset length, m
$\dot{m}$	flow rate, kg/s
n_y	equipment life, year
Pr	Prandtl number,
ΔP	pressure drop, Pa
q	heat transfer rate, W
Re	Reynolds number
s	spacing between adjacent fins, m
S	entropy, J/K

T	Temperature
U	overall heat transfer coefficient, W/m^2.K
V	velocity, m/s
$\dot{V}$	volume flow rate, m^3/s
$\dot{W}_p$	blower work, kW
X	exergy, kW
X_D	exergy destruction, kW
$\dot{Z}$	the annual rate of capital investment, $/y

Greek Symbols

Λ	operation hours, hour
β	the ratio of total heat transfer area to the volume between plates, m^2/m^3
δ	fin metal thickness, m
δ_w	plate thickness, m
ε	Effectiveness
ρ	density, kg/m^3
μ	viscosity, Pa.s
ζ	Fin surface geometry type
η	Efficiency

Subscripts

0	dead state
A	air
c,i	cold in
c,o	cold out
f	fin
fr	frontal
g	gas
h,i	hot in
h,o	hot out
i	in
max	maximum
min	minimum
o	outlet
p	plates
ref	reference
W	wall or window

the empty duct. Similarly, Aliabadi et al [13], investigated three passive techniques to enhance the wavy plate-fin heat exchanger (WPFHX) and reported winglets WPFHX has a maximum performance factor of 1.26 compared to the conventional one. Jiang et al. [14] studied the CHE with offset strip fins for cryogenic helium and reported the most influential parameters to be fin space, thickness, and Reynold number for optimal performance.

Besides, the numerical optimization of heat exchangers has also been proven to be an effective approach for overall performance improvement through re-adjustment of operating and design parameters [18]. For instance, peng and ling [7] using neural networks cooperated with genetic algorithms for the optimization of PFHX and optimization the annual cost by ~45%. Xie et al. [15] used a genetic algorithm for the cost, volume, and pressure drop optimization of PFHX and reported that the cost is reduced ~16%. Sanaye and Hajabdollahi [16] used multi-objective optimization for the PFHX and reduced the cost by 18%. Hu et al. [17] used the sine cosine algorithm to optimize the design of PFHX and reported that the optimum entropy generation unit is 0.0783. Ahmadi et al. [18] employed a multi-objective genetic algorithm to optimize these heat exchangers exegetic and economic performance. They reported that a higher exergy efficiency leads to efficient heat exchangers from the thermo-economic standpoint and fin pitch and

height are the major design parameters. Jamil et al. [19] used a genetic algorithm and reduced the cost of shell and tube heat exchangers by ~20%. Jamil et al. [20] optimized the plate heat exchanger and reduced the cost by ~53%. Raja et al. [21] proposed a many objective (four objectives) algorithm and compared it with a multi-objective (two objective) algorithm to optimize different design variables of a PFHE. They reported that the proposed method optimizes the design variable more accurately as they are close to the decision-making selected point compared to conventional techniques. Banooni et al. [22] used the bee algorithm for the optimization of PFHX and optimum the total cost per year by ~87%. A similar study by Zarea et al. [23] studied the application of a Bees Algorithm Hybrid with Particle Swarm Optimization (BAHPSO) on the PHEs. Their study presented high-level accuracy and efficiency because of the low total annual cost (938.9 $/year) and high effectiveness (0.9385) compared to Jaya algorithm.

The literature review suggests that most of the studies presented above are limited to conventional thermal-hydraulic analysis and very few studies are reported on the economic aspects. The rigorous heat exchanger design and optimization studies covering thermal, hydraulic, exergy, sensitivity, and economic aspects for different fin surfaces are not available. Therefore the current study is focused on adding value to the existing literature by achieving the following objectives (a) a

detailed thermohydraulic heat exchanger design for heat transfer coefficients, pressure drops, pumping power, etc. for different fin geometries, (b) exergy and economic analyses using conventional economic as well as advanced exergo-economic approaches, (c) a thorough parametric analysis using a meticulous normalized sensitivity and one factor at a time approaches, and (d) an economic optimization using Genetic Algorithm.

Materials and methods

Heat exchanger configuration and design

The plate-fin heat exchangers (PFHXs) are used in power plants as energy recovery units as illustrated in Fig. 1. PFHXs recover waste energy and are supplied where required. The system considered consists of a single pass crossflow plate-fin heat exchanger employed for air preheating by recuperating energy from a waste heat stream coming from a cogeneration plant [24]. Two centrifugal fans rated to maintain the flow

Table 1
Specifications of the heat exchanger setup with basic surface characteristics for an offset strip fin surface (1/8–19.86) [25].

Parameter	Value
Process	
Volume flow rate (gas/air), m^3/s	3.494/ 1.358
Inlet temperature (gas/air), °C	900/200
Inlet pressure (gas/air), kPa	160/200
Geometric	
Hot flow length of HX, L_1, m	0.3
Cold flow length of HX, L_2, m	0.3
Non-flow length of HX, L_3, m	1.0
Plate spacing/Fin height, b, m	0.00249
Fin offset length, l_s, m	0.00318
Hydraulic diameter, D_h, m	0.00154
Fin metal thickness, δ, m	0.000102
The ratio of fin area to the total area, A_f/A	0.785
The ratio of total heat transfer area to the volume between plates, β, m^2/m^3	2254
Plate thickness, δ_w, m	0.0005

rate and pressure are integrated with the HX for a complete plant layout, as shown in Fig. 2. For preliminary design and analysis, the process and design parameters comprising of temperatures, flow rates, and geometric specifications are taken from the literature [25] as summarized in Table 1. These parameters are selected from the literature for initial validation [1,16,25–27].

The design of the heat exchanger involves a calculation of heat transfer coefficients (h_g and h_a), pressure drops (ΔP_g and ΔP_a), and overall heat transfer coefficient (U) [28]. In the present study, the ε-NTU approach is used to predict the performance of PFHE. The PFHE is assumed to be running under a steady state, and the area distribution and heat transfer coefficients are considered uniform and constant. The number of passages for the gas side is assumed to be one passage less than airside passages. Table 2 presents the thermal and hydraulic model formulation of PFHE.

Fig. 1. Energy recovery in power plants using a compact heat exchanger.

Fig. 2. Schematic of heat exchanger configuration considered [18,25].

Table 2
Modeling equations for PFHE with offset strip fin ($\zeta = 1/8$–19.86) [16,25].

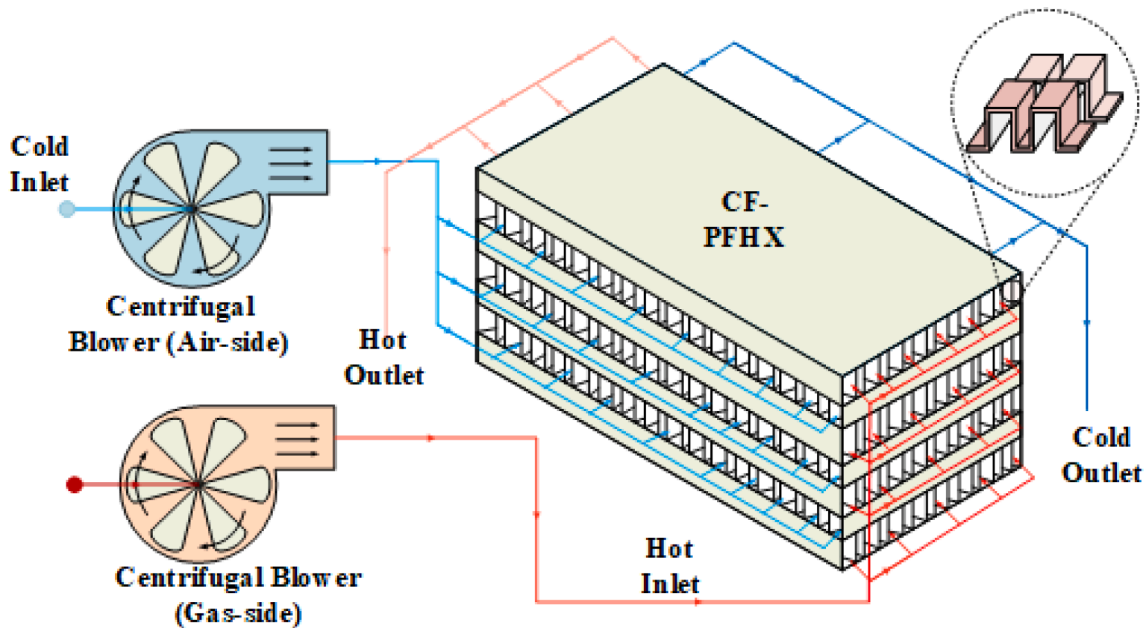| Parameter	Equation	No.
Heat capacity ratio and number of transfer units	$C^* = \dfrac{C_{min}}{C_{max}}, NTU = \dfrac{UA}{C_{min}}$	(1)
The outlet temperature of fluids	$T_{a,o} = T_{a,i} + \dfrac{q}{C_a}, T_{g,o} = T_{g,i} - \dfrac{q}{C_g}$	(2)
Heat transfer rate	$q = \varepsilon \left(T_{g,i} - T_{a,i}\right) C_{min}$	(3)
Heat transfer area	$A_g = \beta_g V_{p,g}, A_a = \beta_a V_{p,a}$	(4)
Frontal area	$A_{fr,g} = L_2 L_3, A_{fr,a} = L_1 L_3$	(5)
The minimum free flow area	$A_{a,g} = \dfrac{(D_h A)_g}{4\ L_g}, A_{a,a} = \dfrac{(D_h A)_a}{4\ L_a}$	(6)
The Colburn factor for offset strip fin	$j = 0.6522Re^{-0.5403}\left(\dfrac{s}{H}\right)^{-0.1541}\left(\dfrac{\delta}{\ell_s}\right)^{0.1499}\left(\dfrac{\delta}{s}\right)^{-0.0678}$ $\times\left[1+5.269\times10^{-5}Re^{1.340}\left(\dfrac{s}{H}\right)^{0.504}\left(\dfrac{\delta}{\ell_s}\right)^{0.456}\left(\dfrac{\delta}{s}\right)^{-1.055}\right]^{0.1}$ $120 < Re < 10^4$	(7)
Fanning friction factor for offset strip fin	$f = 9.6243Re^{-0.7422}\left(\dfrac{s}{H}\right)^{-0.1856}\left(\dfrac{\delta}{\ell_s}\right)^{0.3053}\left(\dfrac{\delta}{s}\right)^{-0.2659}$ $\times\left[1+7.669\times10^{-8}Re^{4.429}\left(\dfrac{s}{H}\right)^{0.920}\left(\dfrac{\delta}{\ell_s}\right)^{3.767}\left(\dfrac{\delta}{s}\right)^{0.236}\right]^{0.1}$ $120 < Re < 10^4$	(8)
Reynolds number	$Re = \dfrac{GD_h}{\mu}$ where $G = \dfrac{\dot{m}}{A_a}$	(9)
Heat transfer-coefficient	$h = \dfrac{jGc_p}{Pr^{\frac{2}{3}}}$	(10)
Pressure drop (air/gas sides)	$\Delta P_{a/g} = \dfrac{G^2}{2g_c\rho_{i,a/g}}\left[\begin{array}{l}\left(1-\sigma^2+K_c\right)+2\left(\dfrac{\rho_{i,a/g}}{\rho_{\circ,a/g}}-1\right)+\\ f\dfrac{L}{r_h}\rho_{i,a/g}\left(\dfrac{1}{\rho_{a/g}}\right)_m - \left(1-\sigma^2-K_c\right)\dfrac{\rho_{i,a/g}}{\rho_{\circ,a/g}}\end{array}\right]$	(11)

Exergy and economic analysis

In addition, the heat exchanger is examined using the Second Law of thermodynamics to estimate the system irreversibility [29]. For this, the exergy destruction is calculated by applying the general exergy balance given for HX in Eq. (12) and the blower in Eq. (13).

$$X_{D,PFHE} = X_{a,i} + X_{g,i} - X_{a,o} - X_{g,o} \tag{12}$$

$$X_{D,B} = X_{w,i} + \dot{W}_{B,i} - X_{w,o} \tag{13}$$

The stream exergy is calculated using the respective flow rate, enthalpy, and entropy as [19].

$$X = \dot{m}\left[\left(h^{'} - h^{'}_0\right) - T_0(s - s_0)\right] \tag{14}$$

The economic analysis involves the calculation of the capital and operational expenses of the system [30]. For the capital cost, the correlations presented in the literature are used for blower and heat exchangers as given in Eqs. (15) to (20) [31].

$$C_{inv,Blower} = C_{index}K^{'}\dot{V}^n \tag{15}$$

$$K = \frac{C_{inv,Ref}}{\dot{V}_{Ref}} \tag{16}$$

where $\dot{V}$, $K^{'}$, and n is the volume flow rate, reference cost const, and exponent of cost, respectively. Furthermore, it is important to mention that the correlations used above for the cost analysis were developed back in years. The correlations predict the cost with accuracy and precision only for the time they were developed [32]. Therefore, cost indices are used to accommodate the market variation and inflation to implement the cost correlation in current times [33]. For this purpose, the idea of using a cost index factor (C_{index}) has been adopted [19,34,35] and the values for C_{index}, $C_{inv,ref}$, $V_{ref.}$ and n are adapted from [31,36].

While for heat exchangers, the capital cost is mainly dependent upon the heat exchanger investment cost per unit area (C_A), effective area (A),

and cost constant (n). The correlation used for the capital cost of PFHE ($C_{in,HX}$) is given as [15].

$$C_{inv,HX} = C_A A^n \tag{17}$$

The operational cost is calculated using current annual cost C_o ($/y), unit energy price C_{elec} ($/kWh), equipment life, n_y (year), operational availability Λ (*hour*), annual inflation rate, i (%), and energy consumption/power of the blower, *BP* (kW) as.

$$C_{op} = \sum_{j=1}^{n_y} \frac{C_o}{(1+i)^j} \tag{18}$$

$$C_o = \left(\frac{\dot{m}_a\,\Delta p_a}{\rho_a} + \frac{\dot{m}_g\,\Delta p_g}{\rho_g}\right)\times\frac{1}{\eta}\times C_{elec}\times\Lambda \tag{19}$$

The values of economic parameters are taken as $n_y = 10$ year, $= 5000\ h/y$, $i = 10\%$, $C_{elec} = 0.02$ ($/kWh) and $\eta = 60\%$ [22].

Finally, the stream cost is calculated using the capital cost rate of the component and cost rate of all the inlet and outlet streams as given below [37,38].

$$\dot{C}_o = \Sigma\,\dot{C}_i + \lambda \tag{20}$$

The capital cost rate of each component is calculated as [39,40]:

$$\lambda = C_{inv}\times\frac{i\times(1+i)^{n_y}}{(1+i)^{n_y}-1}\times\frac{1}{3600\,\Lambda} \tag{21}$$

The respective cost balance equations for blower and heat exchanger are given as:

$$\dot{C}_o = \dot{C}_i + C_{elec}\,\dot{W}_{Blower} + \lambda_{Blower} \tag{22}$$

$$\dot{C}_{c,o} = \dot{C}_{c,i} + \dot{C}_{h,i} - \dot{C}_{h,o} + \lambda_{PFHE} \tag{23}$$

The additional auxiliary equation to solve heat exchanger cost balance is given as [41,42].

$$\frac{\dot{C}_{h,i}}{X_{h,i}} - \frac{\dot{C}_{h,o}}{X_{h,o}} = 0 \qquad (24)$$

Sensitivity analysis

Sensitivity analysis is an important tool to predict a model's most influential and responsive parameters [43]. This technique is beneficial as it improves system performance and highlights the critical areas for future research [44]. Calculus-based sensitivity analysis is the most reliable method to identify the essential input parameters [45]. Recently modified techniques known as Normalized Sensitivity Coefficient (NSC) and Relative Contribution (RC) is an easy and extensive way to find the uncertainty of the model and dominant uncertainty contribution of the model against different input parameters [46]. The NSC is a flexible way as it allows the one-by-one comparison of parameters.

The working of NSC is illustrated in Fig. 3, which involves the selection of output performance parameters and the input parameters. After that, the perturbation (usually taken as ± 1%) of the nominal value of the input parameters is selected. Then, the partial derivate is calculated concerning different input parameters followed by the sensitivity Coefficient (SC) calculation for all performance parameters. The third step calculates the total uncertainty and normalized sensitivity using the given formulae (refer to Fig. 3. Finally, the NSC and RC are calculated for which a detailed procedure is shown in Fig. 2 [19,20].

Numerical solution strategy

The heat exchanger was numerically solved using the above model for thermal, hydraulic, exergy, and economic analyses. These equations were modeled in Engineering Equation Solver (EES) software. In the first step, inlet temperatures, pressures, volume flow rates, and typical values of geometrical parameters for a rectangular offset strip fin $\zeta = 1/$

8–19.86 [1] were provided as input data. Then the numerical model was modified to study three different commercially available offset strip fin geometries, i.e., (ζ = 1/8–19.86, 1/8–15.61, and 1/9–22.68). The thermophysical properties and geometry-dependent factors such as j and f were calculated using the EES internal library routines. After that, the values of thermal performance parameters such as NTU, local, global heat transfer coefficient, heat duty, pressure drops, and economic parameters were calculated. Finally, the Genetic Algorithm (GA) was employed to optimize the HX design for minimum cost.

The numerical code was validated with the literature [25], followed by a comprehensive thermal, hydraulic, exergetic, and exergo-economic analysis. The assumptions steady-state operation, uniform and constant area distributions, uniform heat transfer coefficients were taken for the solution. The solution flow diagram is shown in Fig. 4.

Results and discussion

Numerical model validation and preliminary analysis

The literature validated the numerical model for $\zeta = 1/8$–19.86 with the rating problem for crossflow PFHE [16,25]. The difference between the values obtained from the EES model and literature is presented in Table 3. The results obtained with the developed EES model were satisfactorily close to those presented in the literature with a maximum discrepancy of ± 7.8%. Meanwhile, it is worth mentioning that the values for j and f factor and ε-effectiveness for respective fin geometry of PFHE were accessed directly from the EES software library because of higher accuracy. Moreover, the equations of exergy, economics, and advanced economics were coupled with the initial design equations. So the initial thermohydraulic design of the heat exchanger was conducted first. However, the data set produced by this analysis may be subsequently used for design and performance evaluation of different
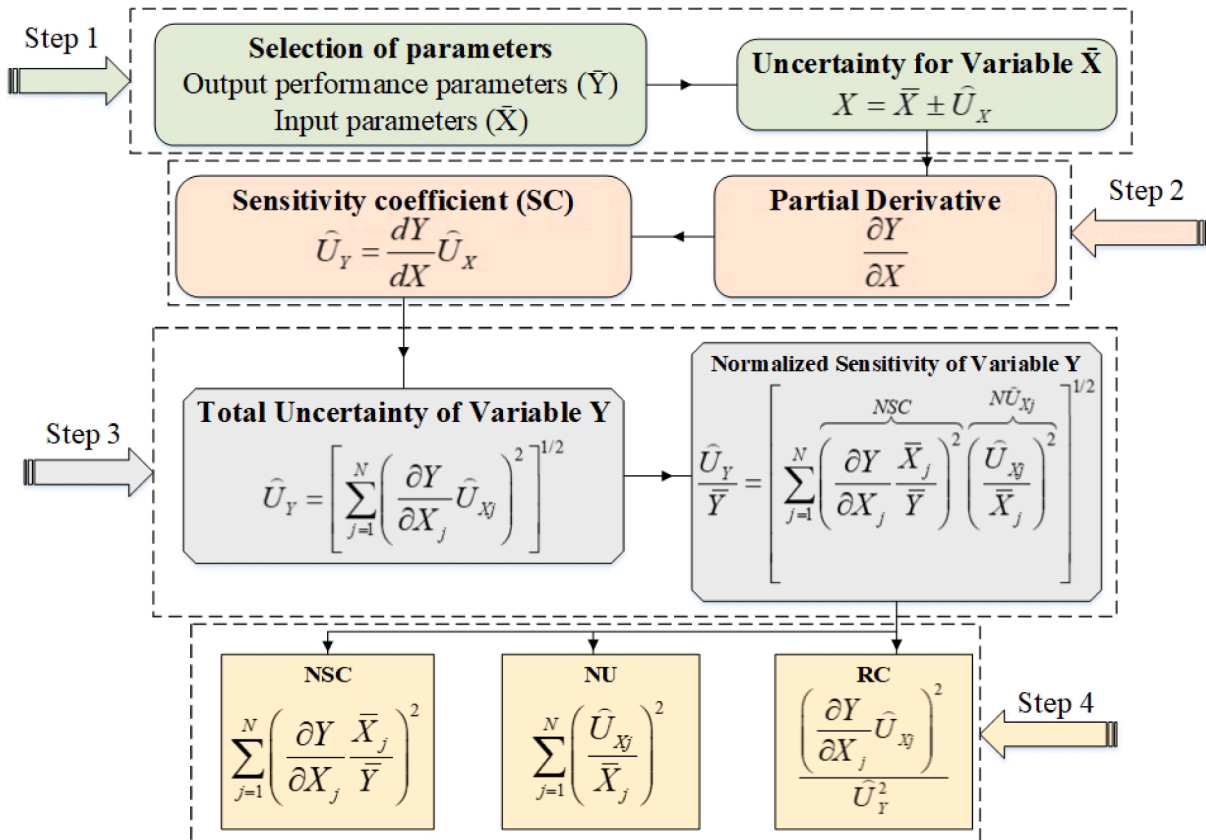

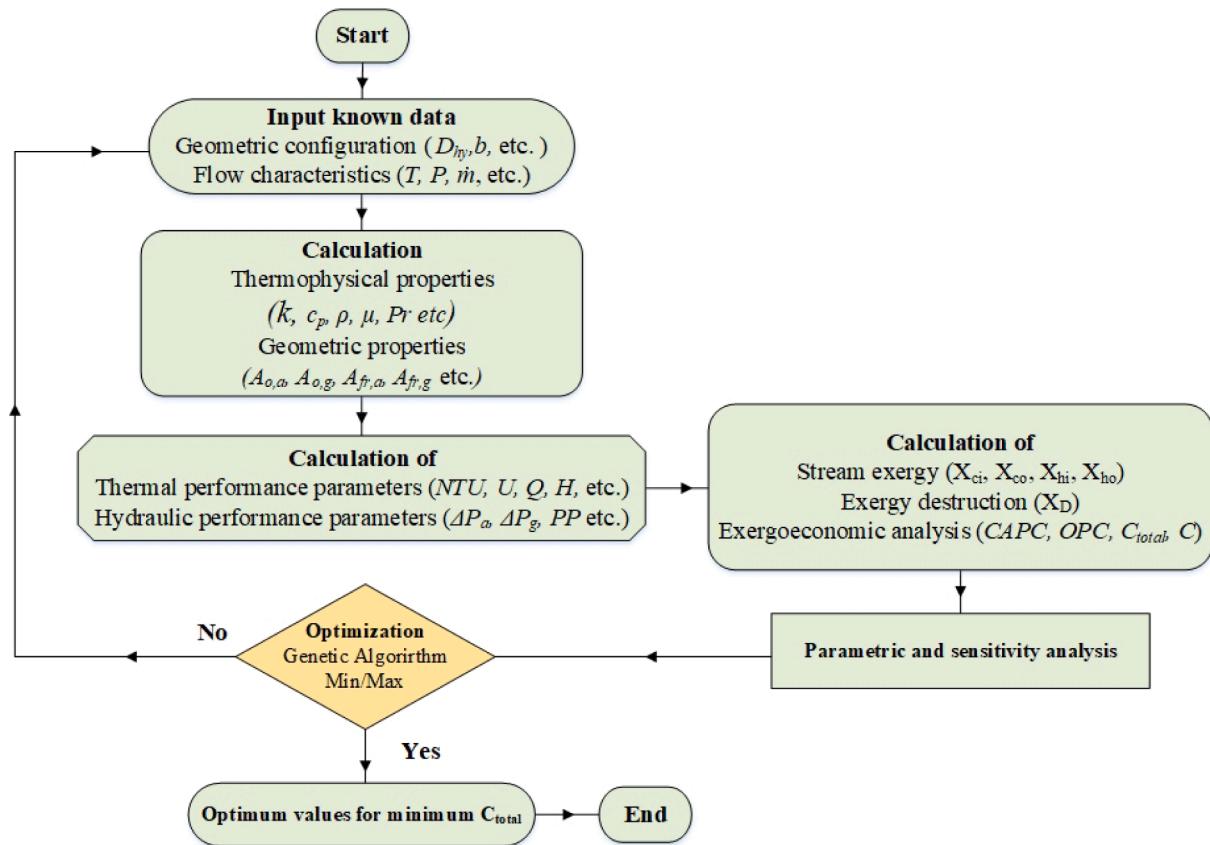**Fig. 3.** Working procedure of normalized sensitivity analysis.

Fig. 4. Solution flow chart.

Table 3
Validation of EES numerical code with literature (for $\zeta = 1/8$–19.86).

Parameter		Current study	Literature [16]	Literature [25].	Error %
Pressure drop (*Pa*)	Gas	9021	8706	9031	0.1–4.4
	Air	8345	8134	8394	0.5–2.5
Heat transfer coefficient $W/(K. m^2)$	Gas	350.5	370.50	360.83	2.8–5.7
	Air	344.1	371.49	336.81	2.1–7.8
Outlet temperature (*K*)	Gas	597.1	–	591.5	0.94
	Air	973.3	–	978.2	0.5

Table 4
A preliminary design with three plate-fin surface geometries for an air to air crossflow plate-fin heat exchanger.

Parameter	Plate fin surface geometry (ζ)		
	1/8–19.86	1/8–15.61	1/9–22.68
Airside heat transfer area, m^2	85.35	66	89.66
Airside Reynolds number	830	1073	790.1
Airside heat transfer coefficient, $W/(m^2K)$	344.1	301.6	305.7
Gas side Reynolds number	576.8	751.6	554.7
Gas side heat transfer coefficient, $W/(m^2K)$	350.5	309.9	336.7
Overall heat transfer coefficient, $W/(m^2K)$	152.5	92.99	78.95
Air side pressure drop, *Pa*	8345	3951	5911
Gas side pressure drop, *Pa*	9021	4228	6731
Air side performance parameter, (*m/s/K*)	0.04123	0.07634	0.05171
Blowing power (*kW*)	71.42	33.57	52.57
Total exergy destruction (*kW*)	148	136.3	149.9
Investment cost of heat exchanger ($)	2205	1890	2271
Total investment cost ($)	2345	2039	2420
Total annual capital investment rate ($/h)	0.07662	0.06636	0.07878
Operating cost ($)	43,883	20,625	32,304
Total cost ($)	44,242	20,933	32,674
Air side product cost ($/h)	1.313	0.6141	0.9474

operational conditions using other algorithms like AI, machine learning where the initial design is not required.

The current study presents a comparison between output values for three different plate-fin surface geometries ($\zeta = 1/8$–19.86, 1/8–15.61, and 1/9–22.68) as shown in Table 4. The heat transfer area for the airside (A_a) appeared to be different for all fin types because it depends directly on the heat exchanger volume between plates, calculated using the plate spacing. Since $\zeta = 1/9$–22.68 has a larger plate spacing than the rest of the two, it has a higher value of heat transfer area. Similarly, Reynold's number is dependent on the hydraulic diameter.

The heat transfer coefficient values depend upon the Colburn factor (j), specific heat and mass flow rates of respective fluids, etc. Since the values of j and f factors changed with fin surface geometry, the heat transfer coefficient values varied accordingly. Moreover, the pressure drop values also changed with the change of fin surface geometry which is evident from their correlations in Table 2. It was mainly due to the Fanning friction factor (*f*) in the correlation of pressure drop. Overall, the change of fin surface geometry somehow affected almost all the important parameters used to model a PFHE.

Sensitivity analysis

The sensitivity analysis for NSC and RC for CF-PFHX with fin configuration ($\zeta = 1/8$–19.86) was conducted for the five output parameters (i.e., U, h_a, ΔP_a, C_{op}, and $\dot{C}_{a,o}$). The input parameters, i.e., process parameters (V_g, V_a, $T_{a,i}$, $T_{g,i}$) and design parameters (L_1, L_2, L_3, δ) were considered for sensitivity analysis. The results are summarized in Tables 5-9. Table 5 highlights the sensitivity of the overall heat transfer

Table 5
The sensitivity of the overall heat transfer coefficient (U) to different parameters.

Variable	U''_X	$\overline{X}$	NSC	RC (%)	$\Gamma\downarrow$	U''_{Total}
V_a	1%	1.358	0.02857	6.818	L_3	0.9871
V_g	1%	3.494	0.07749	18.496	V_g	
$T_{a,i}$	1%	473	0.00154	0.367	L_1	
$T_{g,i}$	1%	1173	0.00027	0.065	L_2	
L_1	1%	0.3	0.05288	12.622	V_a	
L_2	1%	0.3	0.04725	11.278	δ	
L_3	1%	1	0.19714	47.053	$T_{a,i}$	
δ	1%	0.000102	0.01382	3.299	$T_{g,i}$	

Table 6
The sensitivity of the local heat transfer coefficient of airside (h_a) to different parameters.

Variable	U''_X	$\overline{X}$	NSC	RC (%)	$\Gamma\downarrow$	U''_{Total}
V_a	1%	1.358	0.1438	19.73	L_1	2.94
V_g	1%	3.494	0.0187	2.56	L_3	
$T_{a,i}$	1%	473	0.0305	4.19	V_a	
$T_{g,i}$	1%	1173	0.0085	1.17	$T_{a,i}$	
L_1	1%	0.3	0.2663	36.55	V_g	
L_2	1%	0.3	6.50×10^{-35}	8.93×10^{-33}	$T_{g,i}$	
L_3	1%	1	0.2607	35.78	L_2	
δ	1%	0.000102	0	0	Δ	

Table 7
The sensitivity of the pressure drop of airside (h_a) to different parameters.

Variable	U''_X	$\overline{X}$	NSC	RC (%)	$\Gamma\downarrow$	U''_{Total}
V_a	1%	1.358	1.3470	29.23	L_3	0.1791
V_g	1%	3.494	0.0873	1.89	V_a	
$T_{a,i}$	1%	473	0.4972	10.79	$T_{a,i}$	
$T_{g,i}$	1%	1173	0.3827	8.31	$T_{g,i}$	
L_1	1%	0.3	0.2184	4.74	L_1	
L_2	1%	0.3	0.0005	0.010	V_g	
L_3	1%	1	2.0747	45.02	L_2	
δ	1%	0.000102	3.15×10^{-9}	6.80×10^{-8}	Δ	

Table 8
The sensitivity of operational cost (C_{op}) to different parameters.

Variable	U''_X	$\overline{X}$	NSC	RC (%)	$\Gamma\downarrow$	U''_{Total}
V_a	1%	1.358	0.2003	2.829	V_g	1.17×10^3
V_g	1%	3.494	3.6157	51.08	L_3	
$T_{a,i}$	1%	473	0.0477	0.674	L_2	
$T_{g,i}$	1%	1173	0.0219	0.3098	L_1	
L_1	1%	0.3	0.3835	5.4186	V_a	
L_2	1%	0.3	0.9883	13.962	$T_{a,i}$	
L_3	1%	1	1.8206	25.722	$T_{g,i}$	
δ	1%	0.000102	7.49×10^{-7}	1.05×10^{-5}	δ	

Table 9
The sensitivity of outlet cost of airside ($\dot{C}_{a,o}$) to different parameters.

Variable	U''_X	$\overline{X}$	NSC	RC (%)	$\Gamma\downarrow$	U''_{Total}
V_a	1%	1.358	0.4525	8.301	V_g	0.03066
V_g	1%	3.494	2.3470	43.05	L_3	
$T_{a,i}$	1%	473	0.0940	1.724	L_2	
$T_{g,i}$	1%	1173	0.0411	0.754	V_a	
L_1	1%	0.3	0.3591	6.589	L_1	
L_2	1%	0.3	0.6687	12.28	$T_{a,i}$	
L_3	1%	1	1.4887	27.31	$T_{g,i}$	
δ	1%	0.000102	2.471×10^{-5}	0.00045	δ	

coefficient with a total uncertainty of $\pm\,0.9871$. It shows that for the given system and chosen parameters, the most influential and critical parameter in NSC was the non-flow length (L_3) with NSC = 0.197. It was followed by the volume flow rate of gas (V_g) > gas flow length (L_1) > airflow length (L_2) > volume flow rate of air (V_a) > fin thickness (δ) > inlet temperature of air ($T_{a,i}$) > inlet temperature of the gas ($T_{g,i}$), respectively. In contrast, the dominant parameters with the highest RC were non-dimension flow length (L_3) with $\sim 47\%$ contribution, as shown in Table 5.

Likewise, Table 6 shows the local heat transfer coefficient (h_a) with a total uncertainty of $\pm\,2.94$. In term of NSC, it was observed that the most critical parameters was L_1 (NSC = 0.2663) followed by $L_3 > V_a > T_{a,i} > V_g > T_{g,i} > L_2 > \delta$ respectively while the non-flow length (L_3) had the highest RC with $\sim 35\%$ contribution. Similarly, Table 7 shows the sensitivity of the pressure drop of the airside (ΔP_a) with a total uncertainty of $\pm\,0.179$. It shows that the most influential parameter in term of NSC was L_3 (NSC = 2.0747) followed by $V_a > T_{a,i} > T_{g,i} > L_1 > V_g > L_2 > \delta$ respectively while the dominant parameters with highest RC was airflow length (L_2) with $\sim 45\%$ contribution. Similarly, Table 8 shows the impact of different parameters on operation cost with a total uncertainty of $\pm\,1167.49$. It can be observed from Table 8, the most crucial parameter with highest NSC was V_g (NSC = 3.6157) followed by $L_3 > L_2 > L_1 > V_a > T_{a,i} > T_{g,i} > \delta$ respectively while the dominant parameters with highest RC were volume flow rate (V_g) with $\sim 51\%$ contribution. Furthermore, Table 9 shows the sensitivity of the product cost of airside ($\dot{C}_{a,o}$) with a total uncertainty of $\pm\,0.03066$. In term of NSC, it was observed that the most critical parameters is V_g (NSC = 2.3470) followed by $L_3 > L_2 > V_a > L_1 > T_{a,i} > T_{g,i} > \delta$ respectively while the V_g showed the highest RC with $\sim 43\%$ contribution.

Parametric analysis

This section involves the investigation of the effects of essential input parameters on the heat exchanger using the OFAT (one-factor-at-a-time) approach. The results are presented combined for three different offset-strip fin surface geometries ($\zeta = 1/8$–19.86, $1/8$–15.61, and $1/9$–22.68) over a range of parameters.

Effect of flow rate
The mass flow rate is one of the most significant process parameters influencing the compact heat exchanger thermal, hydraulic, and economic performance (as indicated in the sensitivity analysis). It was observed that (refer to Fig. 5a an increase in fluid flow rate increased the heat transfer coefficient (h_a) as well as pressure drop (refer Fig. 5b). It occurred because of the increased Reynold number at high flow rates. The comprehensive thermohydraulic performance parameter (i.e., $h/\Delta P$) showed (see Fig. 5c) that the fin with $\zeta = 1/8$–15.61 had the highest performance followed by $\zeta = 1/9$–22.68, and $\zeta = 1/8$–19.86 which decreased by increasing flow rate because of high fold increment in pressure drop compared to heat transfer coefficient. Besides, it is worth mentioning that an increase in flow rate also increased the heat exchanger operational cost because of higher blower power, as shown in Fig. 6a. Consequently, the hot air stream cost increased with increasing flow rate and pressure drop, as illustrated in Fig. 6(b). Also, the operational cost of the heat exchanger is different for different fin geometries and follows the following order $\zeta = 1/8$–19.86 > $\zeta = 1/9$–22.68 > $\zeta = 1/8$–15.61 due to the difference in geometrical parameters.

Effect of plate spacing
Plate spacing/fin height is another crucial geometric parameter affecting the performance of compact heat exchangers. The increase in plate spacing decreased the heat transfer coefficient and pressure drops (refer to Fig. 7a and b). Since the increase in plate spacing increased the heat transfer rate between plates, leading to lowered pressure drop and heat transfer coefficient. Moreover, j and f factors also vary with the
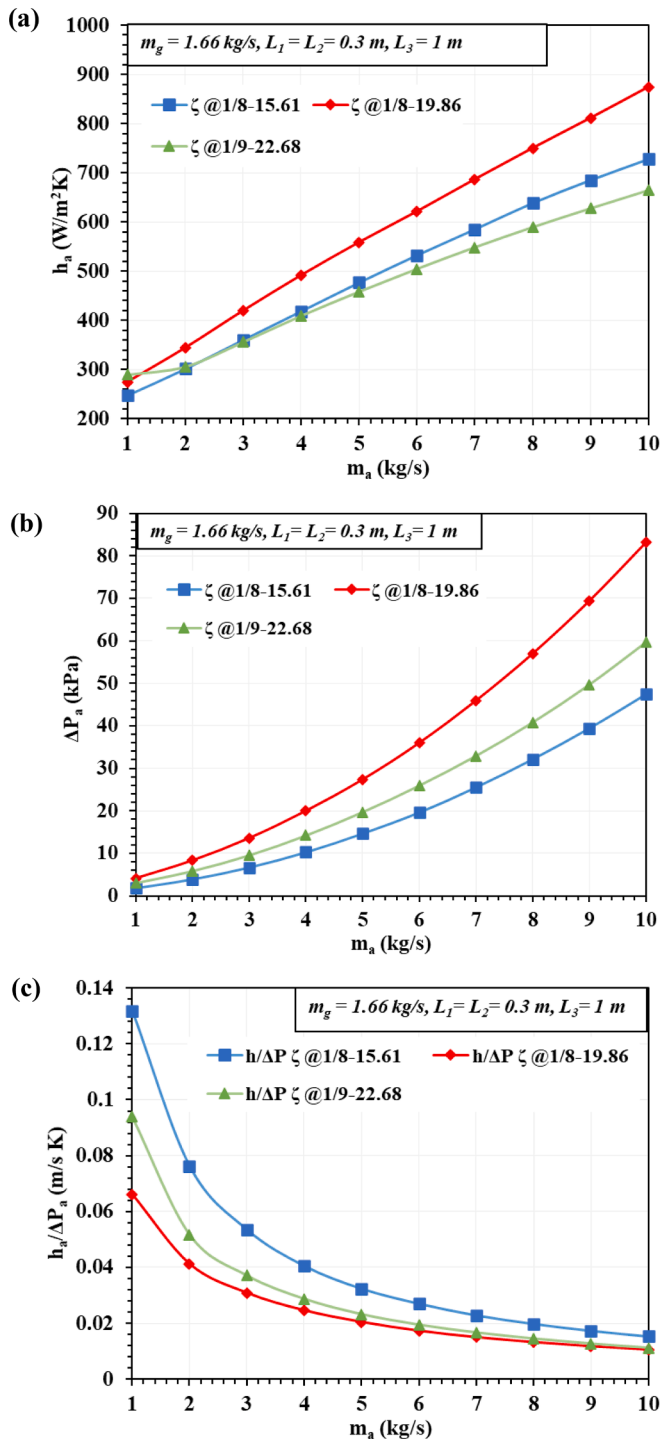
Fig. 5. Effect of airside flow rate on (a) heat transfer coefficient, (b) pressure drop, and (c) h/ΔP.

Fig. 6. Effect of airside flow rate on (a) operational cost, and (b) air outlet stream cost.

variation in plate spacing that significantly affected the h_a and ΔP values. Since the performance parameter ($h_a/\Delta P$) is also influenced by plate spacing i.e.; it increased by increasing the plate spacing as indicated in Fig. 7c. Moreover, plate spacing also affected the economic performance of the compact heat exchangers (refer to Fig. 8a and b). The operational cost was decreased with the increase in plate spacing because of its relation to the decreasing pressure drops. Less blowing power, due to decreased pressure drop, led to lowered operational cost. It was followed by the product cost, which decreased in a similar pattern. It was observed that the operational and product costs varied
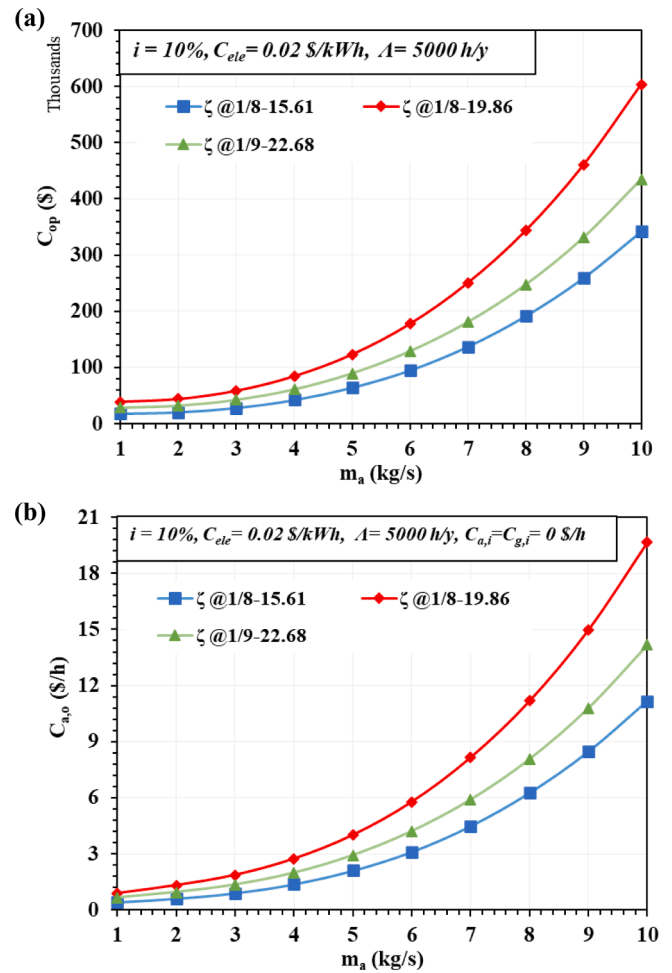
with the variation in fin surface geometry and follow the following order
$\zeta = 1/8–19.86 > \zeta = 1/9–22.68 > \zeta = 1/8–15.61$

Effect of fiscal parameters

The combined analysis of the process parameters and fiscal parameters has become quite significant in thermodynamic systems [35,47]. This is because the systems will have substantially different operational expenses than the conventionally designed heat exchanger [37,39]. In this regard, Fig. 9a demonstrates the effect of the cost index factor (C_{index}) on the investment cost of the heat exchanger. A linear rise in investment cost for each fin surface geometry was observed with the increase of the cost index factor. The investment cost increased ~41.2% for the last 23 years when the cost index factor increased from 1 to 1.7 (for $\zeta = 1/8–19.86$). In Fig. 9b, a linear (though smaller) increase in the product cost of air was observed with an increase in the cost index factor. A similar product cost variation was observed with the interest rate and unit electricity cost, as shown in Fig. 9c and d. For instance, the product cost of cold-water outlet stream showed a significant increase (from 0.5911 to 0.6141 $/h ~ 4%) for a PFHE operating at interest rates of 1% and 10%, respectively (for $\zeta = 1/8–15.61$). It highlights that fiscal parameters are pretty critical for the performance prediction of PFHE.

Exergy-and-cost flow diagram

The exergy-and-cost flow diagram for the heat exchanger configuration considered in this study is presented in Fig. 10. It presents a graphic demonstration of the thermodynamic and monetary performance of the system under consideration at all unique points. In this
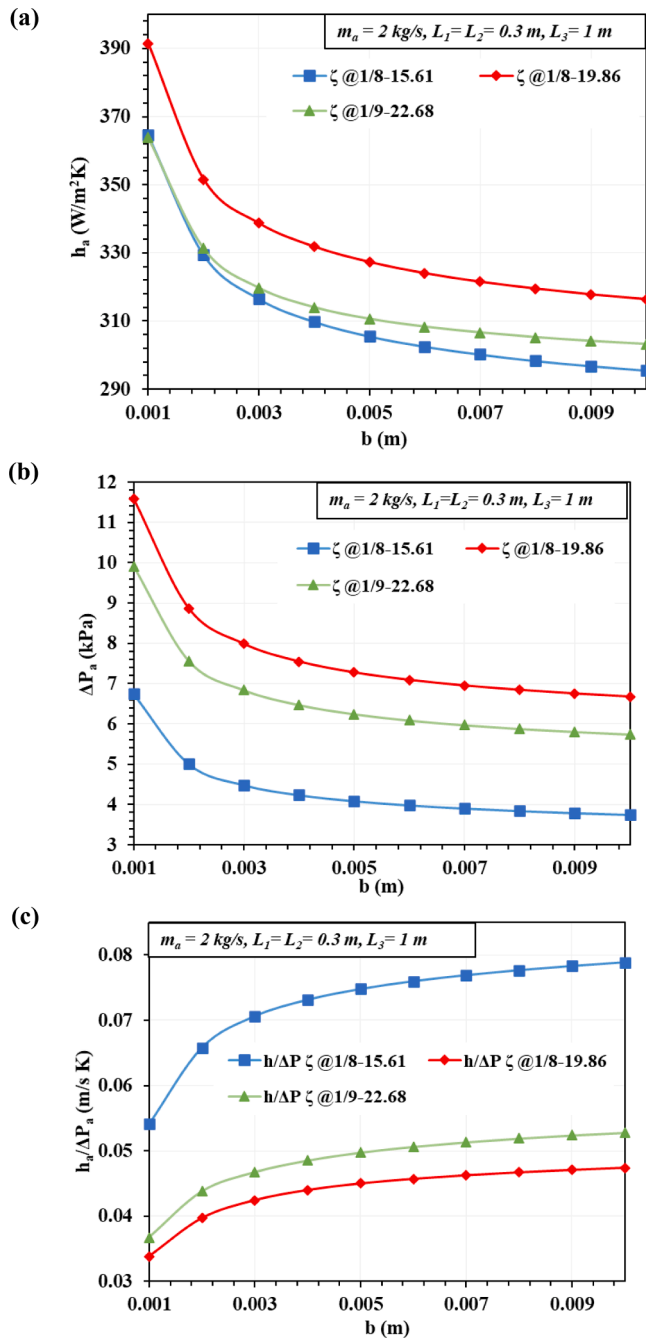
(a)

(b)

(c)

Fig. 7. Effect of fin spacing on airside (a) heat transfer coefficient (b) pressure drop, and (c) h/ΔP.

(a)

(b)

Fig. 8. Effect of fin spacing on (a) operational cost, and (b) airside outlet stream cost.

diagram, the cost (exergy and economic) of all streams in the system at inlets and outlets of the components calculated using fixed and recurring expenses is illustrated. It is significant for the systems with many components (e.g., air separation and liquefaction plants, etc.) and indicates exergy (in kW) and cost rates (in $/h).

Optimization

After a detailed sensitivity analysis using NSC and parametric analysis using OFAT, the CF-PFHX was optimized using the Genetic Algorithm (GA). The details regarding the use of GA for heat exchanger optimization are summarized in a recent study on shell and tube heat exchanger optimization by Jamil et al. [19]. The minimum total cost (C_{total}) and stream cost of CF-PFHX were used as an objective function
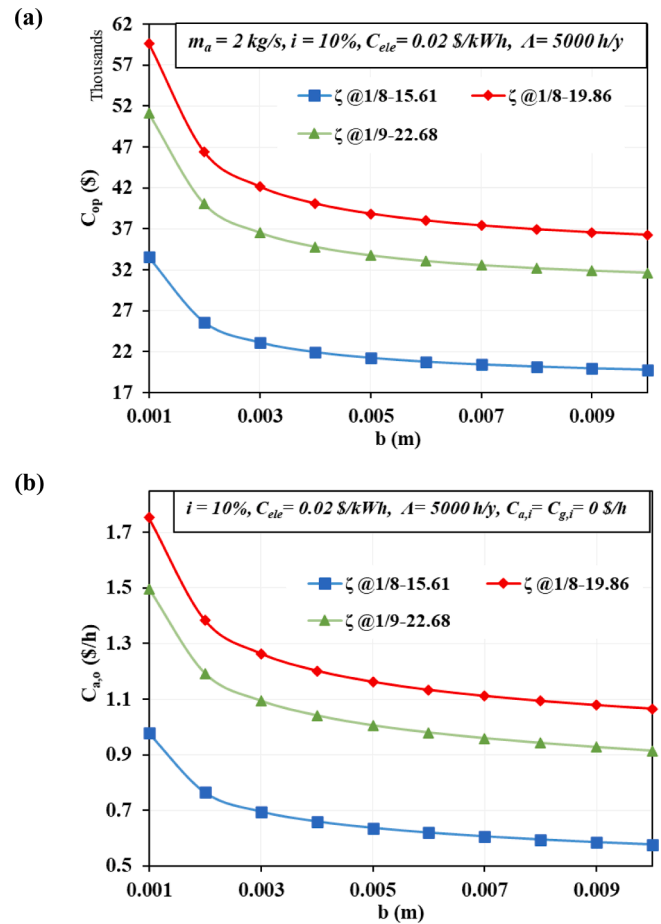
against seven input decision variables such as fin thickness (δ), fin length (l_s), fin spacing (b), lance length ($\bar{l}_a$), hot flow length (L_1), Cold flow length (L_2), non-flow length (L_3). The functional flow diagram of the optimization process is presented in Fig. 11. The currently used optimization technique i.e. Genetic Algorithm picks optimum value from the provided range. However, lower and upper bounds for the range were systematically selected considering different parameters like size, suitability for construction, availability, material characteristics, etc. Despite the fact that some of the parameter values can be obvious to be at a minimum or maximum boundaries, the combinatory effect of their values with other design and process parameters is required to be analyzed for suitable selection. This is what comprehensive numerical study and optimization offer. Moreover, the lower and upper bounds in the current study are selected carefully from the literature [16,22] and summarized in Table 10 while keeping in view the actual available component. The values of algorithm-specific parameters such as generations = 100, population size = 150, and mutation probability = 0.035 are selected carefully from literature [16].

The optimization of CF-PFHX was performed for offset strips with fin frequency (ζ = 1/8–19.86). The standard and optimal values of CF-PFHX (ζ = 1/8–19.86) were summarized in Table 11. It was observed that the optimization significantly improved CF-PFHX performance. For instance, the air and gas side heat transfer coefficient decreased by ~11% and ~69% respectively, while the corresponding pressure drops are also decreased by ~36.9% and ~93.5% respectively, which was favorable for lowering the operational cost. Consequently, the pumping power decreased by ~78.5% due to a reduction in pressure drop. However, the overall comprehensive performance parameter h/ΔP for the air and gas side increased ~40.9% and ~3.78 fold which is very
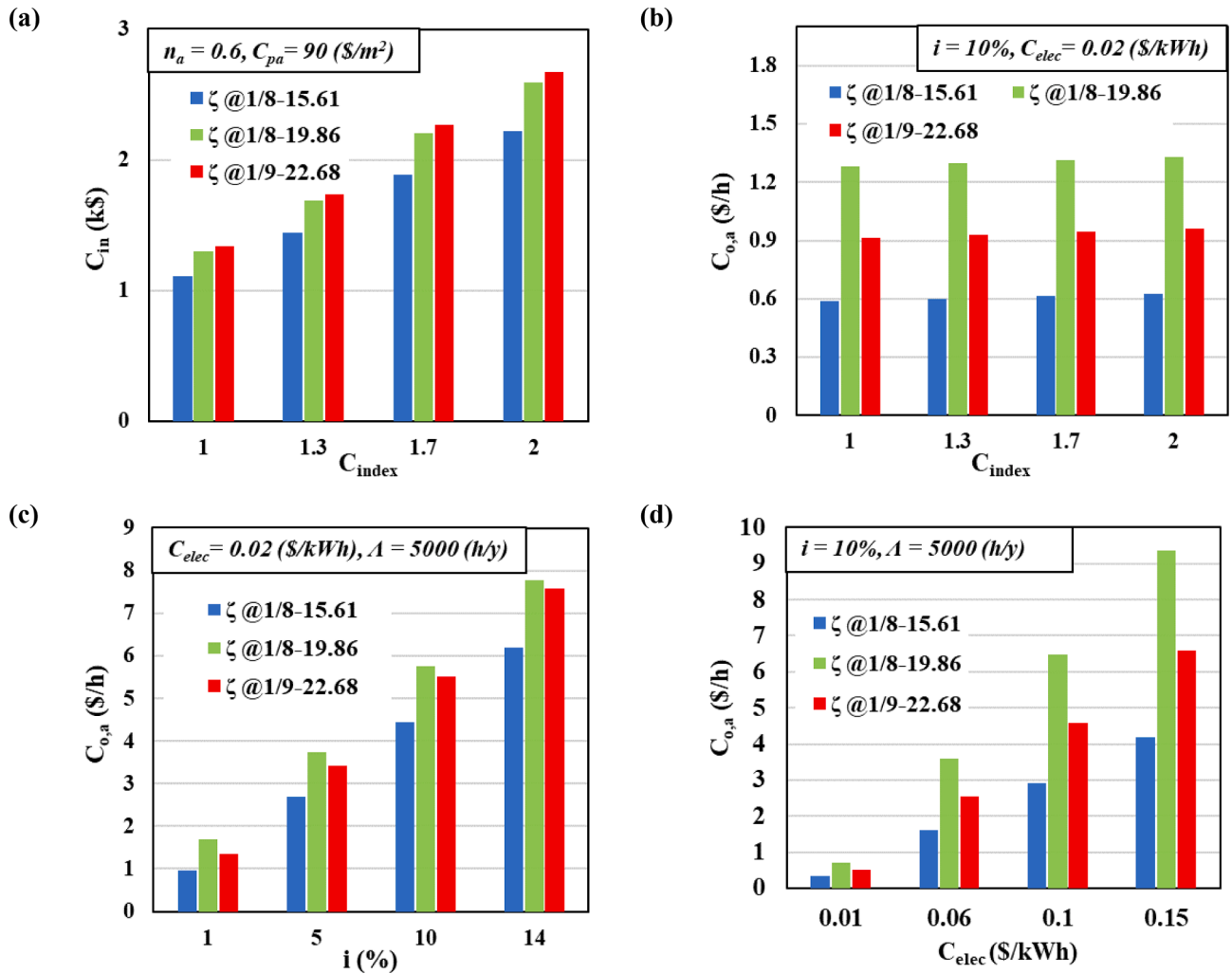
(a)

(b)

(c)

(d)

Fig. 9. Effect of fiscal parameters (a) investment cost versus cost index factor, (b) cold air outlet cost versus cost index factor, (c) cold air outlet cost versus interest rate, and (d) cold air outlet cost versus unit electricity cost.
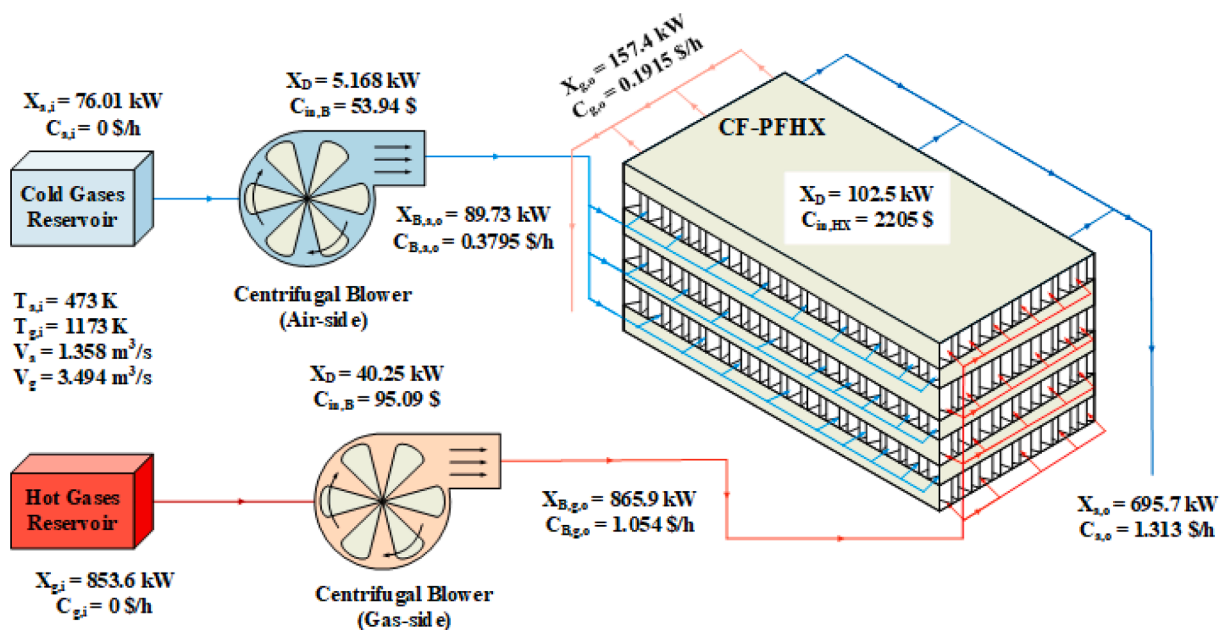

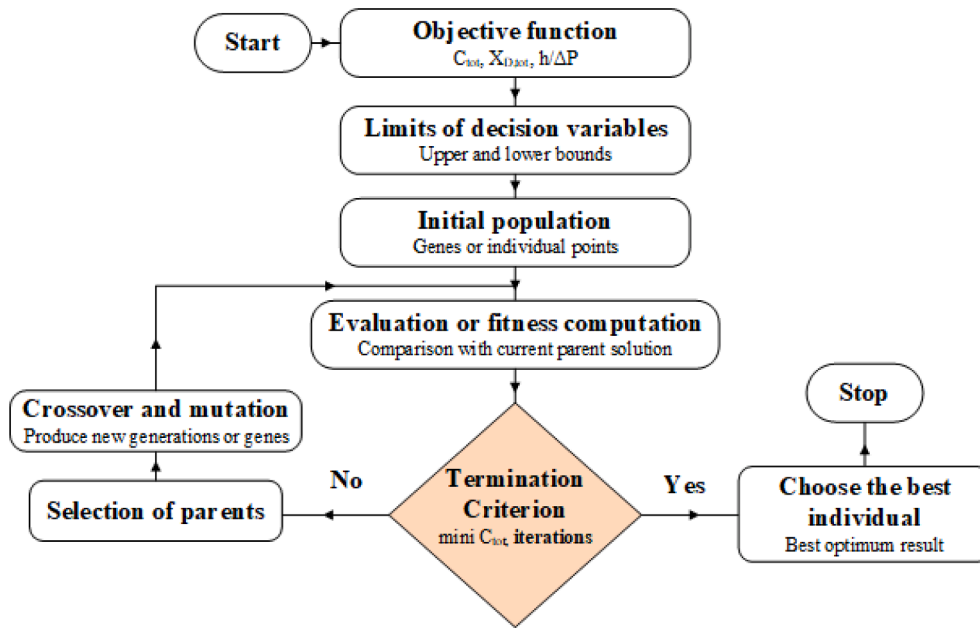**Fig. 10.** Exergy-and-cost flow diagram of the heat exchanger.

Fig. 11. Flow chart of Genetic Algorithm [19].

Table 10

The lower, upper, and optimum value of the design variable for CF-PFHX ($\zeta = 1/8$–19.86) [22].

Parameters	Constraint bounds		
	Lower	Upper	Optimum*
Fin thickness (δ), mm	0.1	0.2	0.10001
Fin length (l_s), mm	2	3.5	2.151
Fin spacing (b), mm	2	10	9.99
Lance length ($\bar{l}_a$), mm	1	10	9.998
Hot flow length (L_1), m	0.1	1	0.2267
Cold flow length (L_2), m	0.1	1	1
Non flow length (L_3), m	0.7	1.2	1.2

* Calculated, note: Not all references provided all data ranges.

Fig. 12. Comparison of operational cost against fin height with literature [22].

significant as the overall CF-PFHX performance is improved. In addition, due to the modification, some decision parameters are increased, such as fin spacing, flow length, which increased the heat transfer area by ~ 3.1 folds resulting in a higher heat transfer rate, lower pressure drop thus reducing the operational cost. Meanwhile, the dominance of the operational cost over the capital cost for long operational life resulted in a

Table 11

Parameters of optimal CF-PFHX ($\zeta = 1/8$–19.86) using a genetic algorithm.

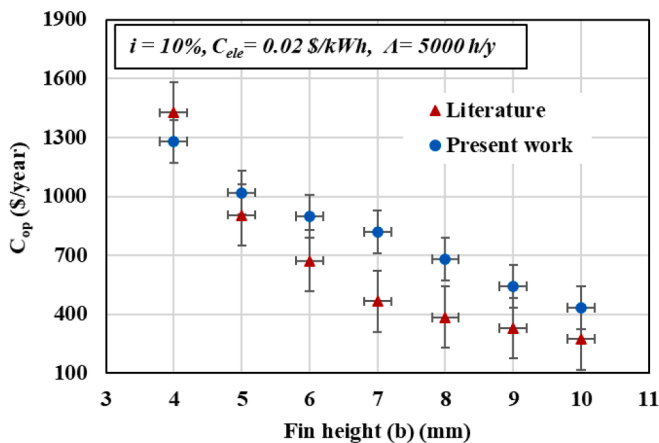| Parameter	Standard [25]	Optimal	Deviation %
Heat duty, kW	1074	1058	1.49 ↓
Airside heat transfer coefficient, $W/(m^2K)$	344.1	306	11.07 ↓
Gas side heat transfer coefficient, $W/(m^2K)$	350.6	108.4	69.08 ↓
Airside pressure drop, kPa	8.345	5.267	36.88 ↓
Gas side pressure drop, kPa	9.021	0.5834	93.53 ↓
Air side performance parameter, $m/(s K)$	0.04123	0.05809	40.89 ↑
Gas side performance parameter, $m/(s K)$	0.03886	0.1858	378.13 ↑
Blowing power, kW	71.42	15.32	78.55 ↓
Total exergy destruction, kW	148	96.15	35.03 ↓
Airside heat transfer area, m^2	85.35	353	313.59 ↑
Investment cost of the heat exchanger, $	2205	5168	134.38 ↑
Operating cost ($), $	43,883	9413	78.55 ↓
Total cost per year, $/year	6851	2234	67.39 ↓
Total cost, $	44,242	10,254	76.82 ↓
Air side product cost, $/h	1.313	0.4657	64.53 ↓

↓: Decrease, ↑: Increase.

decrease in the total cost of the optimized heat exchanger. Similarly, the operational cost was reduced by $\sim 78.5\%$ due to a reduction in pumping power. Finally, the overall results were beneficial as the total annual and total costs for ten years were reduced by $\sim 67.4\%$ and $\sim 76.8\%$, respectively, reducing the air production cost from 1.313 $/h to 0.4657 $/h ($\sim 64.5\%$).

Overall, the cost reduction achieved in the current study with optimization through re-adjustment of design and process parameters is $\sim 67\%$. Compared with the other similar studies, the optimization significantly improved the economic performance of the compact heat exchangers. For instance, Jamil et al. [20] reduced the cost of plate and frame heat exchangers by $\sim 53\%$ using GA. Similarly, for plate-fin heat exchanger, Peng et al. [7] reduced cost by $\sim 45\%$ through ANN, Banooni et al. [22] used Bees Algorithm by 87%, and Yousefi et al. [26] reduced cost by 86% using GA. Finally, the effect of one of the most critical design parameters i.e., plate spacing/fin height (b) on the operational cost as compared with the literature [22]. It was observed (refer to

Fig. 12) that both Bees Algorithm [22] and the current study (based on GA) achieved a reduction in operational cost (C_{op}) through an increase in the fin height. This is because higher fin height resulted in increased spacing between the plates which offered less resistance to the flowing stream; thus, decreasing the pressure drop and power input. The deviation in the magnitude is mainly due to different techniques used with different convergence ratios and operational parameters.

Concluding remarks

A gas-phase (air-to-air) crossflow plate-fin heat exchanger was investigated from thermal, hydraulic, economic, and exergy point viewpoints. The numerical-based thermal-hydraulic model was developed for three different offset-strip fin surface geometries. It was followed by cost-flow and exergy-based analysis for the calculation of fluid stream costs. Normalized sensitivity analysis identified the most influential parameters. In addition, the impact of input parameters was investigated with the help of a detailed parametric study using the one-factor-at-time approach. Finally, the Genetic Algorithm is employed to minimize the total cost of the heat exchanger system under consideration. Some of the core findings of the present study are:

Sensitivity analysis showed the most influential input parameters in terms of NSC for the overall heat transfer coefficient, local heat transfer coefficient, pressure drop, operational cost, and outlet stream cost. These are L_3 (NSC = 0.197), L_1 (NSC = 0.2663), L_3 (NSC = 2.0747), V_g (NSC = 3.6157), and V_g (NSC = 2.3470), respectively.

The parametric analysis showed that the increase of airside mass flow rate increased the heat transfer coefficient, pressure drop, operating and stream costs due to an increase in Reynolds number. Likewise, plate spacing increased heat transfer coefficients, pressure drops, using stream costs on the airside.

Heat exchanger investment and stream cost were significant functions of fiscal parameters like cost index factor, interest rate, and unit cost of electricity.

The optimization of the heat exchanger was carried out by modifying the design parameters. It helped to reduce the operational cost by ~78.5%, total annual cost, and total cost (10 years) by ~67.4% and ~76.8%, respectively, reducing the air production cost from 1.313 \$/h to 0.4657 \$/h (~64.5%).

Declaration of Competing Interest

The authors declare that they have no known competing financial interests or personal relationships that could have appeared to influence the work reported in this paper.

Acknowledgments

References

[1] Kays WMAL. Compact Heat Exchangers. 3rd ed. New York: McGraw-Hill; 1984.
[2] Zhu J, Zhang W, Li Y, Ji P, Wang W. Experimental study of flow distribution in plate–fin heat exchanger and its influence on natural gas liquefaction performance. Appl Therm Eng 2019;155:398–417. https://doi.org/10.1016/j.applthermaleng.2019.04.020.
[3] Xu J-H, Chen X-J, Zhang S-Y, Chen Q-Y, Gou H-W, Tan J-R. Thermal design of large plate-fin heat exchanger for cryogenic air separation unit based on multiple dynamic equilibriums. Appl Therm Eng 2017;113:774–90. https://doi.org/10.1016/j.applthermaleng.2016.10.177.
[4] Boehme R, Parise JAR, Pitanga Marques R. Simulation of multistream plate-fin heat exchangers of an air separation unit. Cryogenics (Guildf) 2003;43(6):325–34. https://doi.org/10.1016/S0011-2275(03)00002-X.
[5] Saggu MH, Sheikh NA, Muhamad Niazi U, Irfan M, Glowacz A, Legutko S. Improved analysis on the fin reliability of a plate fin heat exchanger for usage in lng applications. Energies 2020;13(14):3624. https://doi.org/10.3390/en13143624.
[6] Chennu R, Lewis RW, Massarotti N. Numerical analysis of compact plate-fin heat exchangers for aerospace applications. Int J Numer Methods Heat Fluid Flow 2010;20:897–909.
[7] Peng H, Ling X. Optimal design approach for the plate-fin heat exchangers using neural networks cooperated with genetic algorithms. Appl Therm Eng 2008;28(5-6):642–50. https://doi.org/10.1016/j.applthermaleng.2007.03.032.
[8] Li Qi, Flamant G, Yuan X, Neveu P, Luo L. Compact heat exchangers: A review and future applications for a new generation of high temperature solar receivers. Renew Sustain Energy Rev 2011;15(9):4855–75. https://doi.org/10.1016/j.rser.2011.07.066.
[9] Picon-Nuñez M, Polley GT, Torres-Reyes E, Gallegos-Muñoz A. Surface selection and design of plate-fin heat exchangers. Appl Therm Eng 1999;19(9):917–31. https://doi.org/10.1016/S1359-4311(98)00098-2.
[10] Wen J, Li Y. Study of flow distribution and its improvement on the header of plate-fin heat exchanger. Cryogenics (Guildf) 2004;44(11):823–31. https://doi.org/10.1016/j.cryogenics.2004.04.009.
[11] Yang Y, Li Y. General prediction of the thermal hydraulic performance for plate-fin heat exchanger with offset strip fins. Int J Heat Mass Transf 2014;78:860–70. https://doi.org/10.1016/j.ijheatmasstransfer.2014.07.060.
[12] Khoshvaght-Aliabadi M, Khoshvaght M, Rahnama P. Thermal-hydraulic characteristics of plate-fin heat exchangers with corrugated/vortex-generator plate-fin (CVGPF). Appl Therm Eng 2016;98:690–701. https://doi.org/10.1016/j.applthermaleng.2015.12.135.
[13] Khoshvaght-Aliabadi M, Jafari A, Sartipzadeh O, Salami M. Thermal–hydraulic performance of wavy plate-fin heat exchanger using passive techniques: Perforations, winglets, and nanofluids. Int Commun Heat Mass Transf 2016;78:231–40. https://doi.org/10.1016/j.icheatmasstransfer.2016.09.019.
[14] Jiang Q, Zhuang M, Zhu Z, Shen J. Thermal hydraulic characteristics of cryogenic offset-strip fin heat exchangers. Appl Therm Eng 2019;150:88–98. https://doi.org/10.1016/j.applthermaleng.2018.12.122.
[15] Xie GN, Sunden B, Wang QW. Optimization of compact heat exchangers by a genetic algorithm. Appl Therm Eng 2008;28(8-9):895–906. https://doi.org/10.1016/j.applthermaleng.2007.07.008.
[16] Sanaye S, Hajabdollahi H. Thermal-economic multi-objective optimization of plate fin heat exchanger using genetic algorithm. Appl Energy 2010;87(6):1893–902. https://doi.org/10.1016/j.apenergy.2009.11.016.
[17] Hu T, Zhang L, Yang Z, Guo Y, Ma H. Design optimization of plate-fin heat exchanger using sine cosine algorithm. Commun Comput Inf Sci. 2020. 1265. CCIS. 408–19. https://doi.org/10.1007/978-981-15-7670-6_34.
[18] Ahmadi P, Hajabdollahi H, Dincer I. Cost and entropy generation minimization of a cross-flow plate fin heat exchanger using multi-objective genetic algorithm. J Heat Transfer 2011;133:1–10. https://doi.org/10.1115/1.4002599.
[19] Jamil MA, Goraya TS, Shahzad MW, Zubair SM. Exergoeconomic optimization of a shell-and-tube heat exchanger. Energy Convers Manag 2020;226:113462. https://doi.org/10.1016/j.enconman.2020.113462.
[20] Jamil MA, Goraya TS, Ng KC, Zubair SM, Xu BB, Shahzad MW. Optimizing the energy recovery section in thermal desalination systems for improved thermodynamic, economic, and environmental performance. Int Commun Heat Mass Transf 2021;124:105244. https://doi.org/10.1016/j.icheatmasstransfer.2021.105244.
[21] Raja BD, Jhala RL, Patel V. Many-objective optimization of cross-flow plate-fin heat exchanger. Int J Therm Sci 2017;118:320–39. https://doi.org/10.1016/j.ijthermalsci.2017.05.005.
[22] Banooni S, Zarea H, Molana M. Thermodynamic and Economic Optimization of Plate Fin Heat Exchangers Using the Bees Algorithm. Heat Transf Res 2014;43(5): 427–46. https://doi.org/10.1002/htj.2014.43.issue-510.1002/htj.21087.
[23] Zarea H, Kashkooli FM, Soltani M, Rezaeian M. A novel single and multi-objective optimization approach based on Bees Algorithm Hybrid with Particle Swarm Optimization (BAHPSO): Application to thermal-economic design of plate fin heat exchangers. Int J Therm Sci 2018;129:552–64. https://doi.org/10.1016/j.ijthermalsci.2018.04.009.
[24] Cengel MAB and YA. Thermodynamics: An Engineering Approach. 5. 2016.
[25] Shah RK, Sekuli DP. Fundamental of heat exchanger design. John Wiley & Sons 2003. https://doi.org/10.1002/9780470172605.ch10.
[26] Yousefi M, Darus AN, Mohammadi H. An imperialist competitive algorithm for optimal design of plate-fin heat exchangers. Int J Heat Mass Transf 2012;55(11-12):3178–85. https://doi.org/10.1016/j.ijheatmasstransfer.2012.02.041.
[27] Sanaye S, Hajabdollahi H. Multi-objective optimization of shell and tube heat exchangers. Appl Therm Eng 2010;30(14-15):1937–45. https://doi.org/10.1016/j.applthermaleng.2010.04.018.
[28] Jamil MA, Goraya TS, Yaqoob H, Shahzad MW, Zubair SM. Experimental and Numerical Analysis of a Plate Heat Exchanger Using Variable Heat Transfer Coefficient. Heat Transf Eng 2021:1–13. https://doi.org/10.1080/01457632.2021.1989841.
[29] Tsatsaronis G. Definitions and nomenclature in exergy analysis and exergoeconomics. Energy 2007;32(4):249–53.
[30] Abid A, Jamil MA, Sabah Nu, Farooq MU, Yaqoob H, Khan LA, et al. Exergoeconomic optimization of a forward feed multi-effect desalination system with and without energy recovery. Desalination 2021;499:114808. https://doi.org/10.1016/j.desal.2020.114808.
[31] Turton R, Shaeiwitz JA, Bhattacharyya D. Analysis, Synthesis, and Design of Chemical Processes Fifth Edition. 2018.

[32] Caputo AC, Pelagagge PM, Salini P. Manufacturing cost model for heat exchangers optimization. Appl Therm Eng 2016;94:513–33. https://doi.org/10.1016/j.applthermaleng.2015.10.123.

[33] Zhang C, Liu C, Wang S, Xu X, Li Q. Thermo-economic comparison of subcritical organic Rankine cycle based on different heat exchanger configurations. Energy 2017;123:728–41. https://doi.org/10.1016/j.energy.2017.01.132.

[34] Li J, Yang Z, Hu S, Yang F, Duan Y. Effects of shell-and-tube heat exchanger arranged forms on the thermo-economic performance of organic Rankine cycle systems using hydrocarbons. Energy Convers Manag 2020;203:112248. https://doi.org/10.1016/j.enconman.2019.112248.

[35] Jamil MA, Zubair SM. Design and analysis of a forward feed multi-effect mechanical vapor compression desalination system: An exergo-economic approach. Energy 2017;140:1107–20. https://doi.org/10.1016/j.energy.2017.08.053.

[36] Perry RH, Green DW, Maloney JO. CHEMICAL ENGINEERS' HANDBOOK SEVENTH Late Editor. 1997.

[37] Jamil MA, Zubair SM. On thermoeconomic analysis of a single-effect mechanical vapor compression desalination system. Desalination 2017;420:292–307.

[38] El-Emam RS, Dincer I. Thermodynamic and thermoeconomic analyses of seawater reverse osmosis desalination plant with energy recovery. Energy 2014;64:154–63.

[39] Jamil MA, Zubair SM. Effect of feed flow arrangement and number of evaporators on the performance of multi-effect mechanical vapor compression desalination systems. Desalination 2018;429:76–87. https://doi.org/10.1016/j.desal.2017.12.007.

[40] Nafey AS, Fath HES, Mabrouk AA. Exergy and thermoeconomic evaluation of MSF process using a new visual package. Desalination 2006;201(1-3):224–40.

[41] Rosen M a. A concise review of exergy-based economic methods. Int. Conf. Energy Environ. 2008. 9.

[42] Lazzaretto Andrea, Tsatsaronis George. SPECO: A systematic and general methodology for calculating efficiencies and costs in thermal systems. Energy 2006;31(8-9):1257–89.

[43] Qureshi BA, Zubair SM. A comprehensive design and rating study of evaporative coolers and condensers. Part II. Sensitivity analysis. Int J Refrig 2006;29:659–68.

[44] Kitchell James F, Stewart Donald J, Weininger David. Applications of a Bioenergetics Model to Yellow Perch (Perca flavescens) and Walleye (Stizostedion vitreum vitreum). J Fish Res Board Canada 1977;34(10):1922–35.

[45] Ahmad Jamil Muhammad, Yaqoob Haseeb, Abid Asad, Umer Farooq Muhammad, us Sabah Noor, Bin Xu Ben, et al. An exergoeconomic and normalized sensitivity based comprehensive investigation of a hybrid power-and-water desalination system. Sustain Energy Technol Assessments 2021;47:101463. https://doi.org/10.1016/j.seta.2021.101463.

[46] Masi M, Fogliani S, Carra S. Sensitivity analysis on indium phosphide liquid encapsulated Czochralski growth. Cryst Res Technol 1999;34(9):1157–67.

[47] Jamil MA, Elmutasim SM, Zubair SM. Exergo-economic analysis of a hybrid humidification dehumidification reverse osmosis (HDH-RO) system operating under different retrofits. Energy Convers Manag 2018;158:286–97. https://doi.org/10.1016/j.enconman.2017.11.025.